Cooperative Control Method Based on Two-Objective Optimization for MMCs in HVDC Systems

Jinli Lv , Jiankang Zhang , Yuan Zhi , Kangping Wang , Pengjiang Ge , Jun Zhang , Qiang Li *

Posted Date: 8 May 2025

doi: 10.20944/preprints202505.0544.v1

Keywords: multi-objective optimization; droop control; cooperative control; power sharing; voltage deviation; HVDC systems

 doi:10.20944/preprints202505.0544.v1

Article

Cooperative Control Method Based on Two-Objective Optimization for MMCs in HVDC Systems

Jinli Lv [1], Jiankang Zhang [1], Yuan Zhi [1], Kangping Wang [1], Pengjiang Ge [1], Jun Zhang [2] and Qiang Li [2,*]

[1] Northwest Branch of State Grid Corporation of China, Xi'an 710048, Shaanxi Province, China

[2] State Key Laboratory of Power Transmission Equipment & System Security and New Technology, School of Electrical Engineering, Chongqing University, Chongqing 400044, China

* Correspondence: qiangli@cqu.edu.cn

Abstract: High voltage direct current (HVDC) systems, with its advantages of large capacity, long distance, high efficiency, and low loss, are becoming the core support of the new power system. However, in conventional droop control, the fixed droop coefficient causes output power disproportionate to their available capacities among converters, as well as relatively large deviation of DC voltage in HVDC systems. Therefore, in this paper a two-objective optimization model for droop control is developed and then it is integrated to a cooperative control, which achieves the co-optimization of voltage deviation and power sharing among multiple converters. In the optimization model, there are two objectives, minimization of voltage deviation and maximization of capacity utilization rates of converters. Further, a cooperative control based on optimization model is proposed, where information of voltage and power in droop-controlled converters is acquired and the co-optimization of voltage deviation and power sharing is performed to obtain the optimal droop coefficients for these converters, which minimizes voltage deviation and at the same time make power mismatches proportional to their available capacities among converters. Finally, a testbed is built in PSCAD/EMTDC and three cases are designed to verify the proposed method under different settings. The simulation results show that compared with conventional droop control, the voltage deviation is reduced by 71.74% and 67.67% under the cases of out of service of a converter and the three-phase ground fault of a converter, respectively. Additionally, when large power fluctuations occur twice, the power mismatches are shared proportionally to their available capacities, which results in the capacity utilization rates of the droop-controlled converters increased by 24.46% and 18.75%, respectively.

Keywords: multi-objective optimization; droop control; cooperative control; power sharing; voltage deviation; HVDC systems

1. Introduction

With the rapid development of cross-regional grid interconnections, high-voltage direct current (HVDC) system has emerged as a key component of the modern energy internet, owing to its unique advantages in long-distance and high-capacity power transmission[1]. HVDC systems offer several benefits, including independence from external power sources for commutation, compatibility with weak AC systems, high controllability and flexibility, immunity to commutation faults, and enhanced operational reliability [2-4]. These features make HVDC an efficient solution for connecting asynchronous AC networks and integrating renewable energy sources such as offshore wind farms[5] [6]. In HVDC systems, the application of modular multilevel converters (MMCs) at the receiving end facilitates the implementation of multi-terminal configurations, allowing for decentralized power injection into the AC system. Compared with traditional centralized DC feeding,

 doi:10.20944/preprints202505.0544.v1

this approach enhances the utilization of the receiving grid's transmission capacity and improves feeder reliability. DC voltage droop control, as an adaptive regulation strategy that does not require communication, is widely employed to achieve power sharing and voltage support among multiple converters [7]. It is particularly suitable for controlling multiple MMCs at the receiving end of a hybrid cascade system. Conventional droop control achieves power and voltage regulation through fixed droop coefficients. However, studies have demonstrated that relying solely on empirically tuned fixed coefficients can constrain the operational flexibility of the DC grid[8]. Under DC faults or power fluctuations, such fixed strategies may lead to converter overloads or DC voltage instability, posing challenges to maintaining safe and stable system operation.

Therefore, improving droop control strategies has become a major research focus both domestically and internationally. Wang et al. [9]proposed a voltage droop control strategy based on adaptive reference power. This method compensates for power losses in droop-controlled voltage source converters (VSCs) by adjusting the reference power. Liu et al. [10]introduced a DC voltage restoration strategy, which utilizes the cooperation of multiple converters and dynamic frequency droop coefficients to regulate the support power of the DC grid, ensuring a balance between frequency regulation in the disturbed AC system and voltage stability in the DC grid. Liu et al. [11]proposed a voltage regulation approach based on the joint coordination of centralized optimal control (COC) and adaptive droop control (ADC), which enhances the voltage profile and balances power loading among different VSCs. Sun et al. [12]developed a combined droop control strategy that integrates power/voltage (P/V) and current/voltage (I/V) methods. This strategy enables power redistribution during power disturbances and incorporates excess power reduction mechanisms in the event of converter overload. Ye et al. [13]proposed an improved droop control method, which employs a nonlinear combination of two droop coefficients to reduce system losses and preserve power margins, achieving multi-objective optimal operation across the full voltage range.

However, in the droop control of multiple modular multilevel converters (MMCs), the conflict between voltage and power control—common in conventional multi-terminal DC (MTDC) transmission systems—still arises. Active power distribution and DC voltage control interact through droop coefficients, representing two conflicting control objectives. Optimizing a single droop-controlled converter station alone cannot achieve coordinated operation or global optimization among converters. Beerten and Belmans [14]proposed an optimization algorithm to address the dual objectives of DC voltage regulation and power sharing in VSC-MTDC systems. The algorithm focuses on the selection of droop coefficients and is applicable to both current-based and power-based droop control methods. Gavriluta et al. [15]proposed a decentralized master control layer that combines sag control and DC-Bus signal control. Wang et al. [16]introduced a hierarchical control concept that integrates an integral voltage controller with an average consensus algorithm at the secondary control level. Lee and Kim [17]developed a dynamic droop control strategy based on deep reinforcement learning, featuring centralized training and distributed execution to improve power quality. Gabl et al. [18]proposed a multi-objective integrated secondary and tertiary control method that minimizes losses, voltage deviations, and frequency deviations in microgrid systems. Zhang et al. [19]presented a combinatorial control strategy for accurate power sharing in MTDC systems, operating in both centralized (hierarchical control) and distributed (autonomous control) modes, to minimize DC grid losses and voltage variations.

In summary, existing works have made a lot of efforts on the optimization and control of HVDC systems, but researchers are still in the process of improving their system performances. For example, how could a trade-off between the suppression of DC voltage deviations and the proportional sharing of power mismatches to available capacities be achieved cooperatively? Therefore, the co-optimization of voltage deviation and power sharing should be considered, and a cooperative control method integrated with multi-objective optimization for MMCs in HVDC Systems is proposed. The main contributions of this paper can be summarized as follows.

1. A two-objective optimization model is developed, i.e. minimization of voltage deviation and maximization of capacity utilization rates of converters. Here, the maximization of capacity

 doi:10.20944/preprints202505.0544.v1

utilization rates of converters is achieved, when power mismatches are shared proportionally to their available capacities under the minimization of voltage deviation, where a coefficient for available capacities is constructed to balance these two objectives.

2. A cooperative control integrated the two-objective optimization model is proposed. First, the information of voltage and power among droop-controlled converters is acquired and the co-optimization of voltage deviation and power sharing is performed, where all information is considered cooperatively and solved by the grey wolf optimization (GWO) to obtain the optimal droop coefficients for these converters.

3. A testbed is established in PSCAD/EMTDC and simulations are carried out under different conditions. Compared to conventional droop control, the DC voltage deviation is reduced significantly by 71.74% and 67.67%, when a converter is out of service of and the three-phase ground fault occurs, respectively. Moreover, the capacity utilization rates of the droop-controlled converters increased by 24.46% and 18.75%, respectively.

The remainder of this paper is organized as follows. Section II introduces the structure of the HVDC system and the droop control strategies of the MMCs. Section III introduces the two-objective optimization model and its constraints. Section IV introduces the cooperative control method integrated with the two-objective optimization model and its solutions. Section V establishes a testbed in PSCAD/EMTDC to verify the validity of the proposed strategy. Conclusions are given in Section VI.

2. Model of a HVDC system

2.1. Structure of the System

The structure of the High voltage direct current (HVDC) system is shown in Figure 1. The rectifier-side converter is configured with a line-commutated converter (LCC), while the inverter-side converter features a structure in which an LCC is connected in series with several modular multilevel converters (MMCs). Specifically, the rectifier-side LCC adopts a double 12-pulse configuration, and the inverter-side LCC adopts a single 12-pulse configuration. Each converter can be connected to a different AC bus.

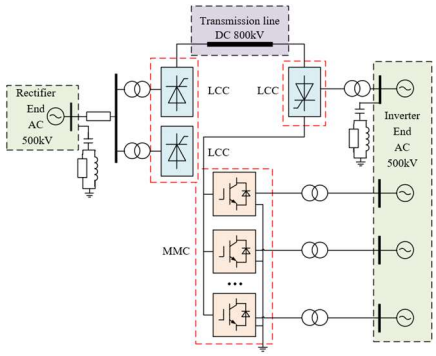

Figure 2. The structure of a HVDC system.

2.2. Droop Control Strategies for MMCs

The P-V droop control is based on the operating curves of DC voltage and active power to realize its active control towards the stable operating point, which can be well adapted to the scenario of frequent fluctuation of active power. When the system is operating in steady state, the relationship between DC voltage and active power at the converter is

$$P_{si} = K_{\text{droop}i}(U_{\text{dcref}} - U_{\text{dc}i}) + P_{\text{sref}i} \tag{1}$$

 doi:10.20944/preprints202505.0544.v1

where U_{dcref} is the reference value of DC side voltage; $U_{\text{dc}i}$ is the actual value of DC side voltage, $P_{\text{sref}i}$ is the reference value of active power, P_{si} is the actual value of active power, $K_{\text{droop}i}$ is the droop coefficient.

Based on equation (1), the droop coefficient can be expressed as:

$$K_{\text{droop}i} = -\frac{P_{\text{sref}i} - P_{si}}{U_{\text{dcref}} - U_{\text{dc}i}} = -\frac{\Delta P_{si}}{\Delta U_{\text{dc}i}} \tag{2}$$

where ΔP_{si} denotes the active power deviation of the converter MMC i and $\Delta U_{\text{dc}i}$ denotes the DC voltage deviation of the converter MMC i.

From Eq. (2), it can be seen that if the droop coefficient is chosen to be larger, the DC voltage control performance is better, but it will lead to poorer active power regulation performance; if the droop coefficient is chosen to be smaller, the active power sharing capability is better, but at this time, smaller power fluctuations will cause a larger DC voltage deviation. The size of the droop coefficient will directly affect the accuracy of DC voltage control and power sharing, and the selection of a suitable droop coefficient can effectively improve the performance of the converter. The outer-loop control structure of the droop controller is shown in Figure 2.

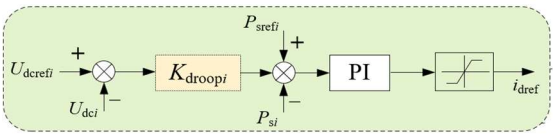

Figure 3. Droop control outer-loop control structure.

3. Two-Objective Optimization Model

Considering the operational characteristics and control requirements of HVDC systems, the optimization model proposed in this paper includes two core objectives: minimization of voltage deviation and maximization of capacity utilization rates of converters. DC voltage stability is crucial for maintaining system energy transmission and equipment safety, as it directly impacts the power regulation capability of each converter. On the other hand, power mismatches sharing is essential to prevent local overload or power redundancy by coordinating the power distribution among multiple converters, thus enhancing the overall controllability of the system. There is a dynamic coupling between the two: adjustments in power sharing may lead to voltage fluctuations, while voltage control depends on the synergistic correction of power sharing. Therefore, achieving a dynamic trade-off between these two objectives through two-objective optimization is necessary.

3.1. Objective 1: Voltage Deviation

DC voltage deviation is a critical concern in HVDC systems. A drop in DC voltage directly impacts the turn-off angle margin of the LCC, significantly increasing the risk of phase change failure. This can lead to a sudden rise in DC current and voltage fluctuations at the AC bus. Moreover, DC voltage fluctuations disrupt the power balance between the receiving end converters. If the DC voltage deviates too far from the desired value, the droop-controlled converters may diverge from the intended power reference, affecting the normal operation of the loads. Voltage instability can also trigger sub-synchronous oscillations between the MMC and the AC power grid. Therefore, minimizing DC voltage deviation is a key objective in the optimization model.

The minimum objective function for voltage deviation is defined as

$$\min \ (U_{\text{dcref}} - U_{\text{dc}i})^2 \tag{3}$$

where n is the number of converters adopting voltage droop control strategy.

 doi:10.20944/preprints202505.0544.v1

3.2. Objective 2: Power Mismatches Sharing

In HVDC systems, it is essential not only to control the power variation of the receiving end converters to ensure that the sum of the deviations between the output power of multiple converters and the reference power is minimized, but also to address the power sharing issue. If the power sharing of the MMCs becomes uncontrolled, leading to a DC voltage drop, the probability of LCC phase change failure significantly increases, and DC blocking may be triggered. When an MMC is withdrawn for maintenance or due to a failure, the remaining converters must redistribute power according to the capacity margin. If the power sharing is uneven, small-capacity MMCs may exceed their limits during peak loads. Additionally, when multiple MMCs are connected in parallel via the DC bus, improper power sharing strategies can lead to low-frequency oscillation issues. Therefore, it is crucial to ensure that the power mismatches are shared proportionally to available capacities of the droop-controlled converters.

Typically, the power margin of a converter is

$$P_{\text{marg}i} = \begin{cases} P_{\max i} - P_{si} & , P_{si} \geq P_{\text{sref}i} \\ P_{si} & , P_{si} < P_{\text{sref}i} \end{cases} \tag{4}$$

In this paper, ω_i is defined as the power margin coefficient of the MMC i, which is expressed as:

$$\omega_i = \begin{cases} \dfrac{P_{\max i}}{P_{\max i} - P_{si}} & , P_{si} \geq P_{\text{sref}i} \\ \dfrac{P_{\max i}}{P_{si}} & , P_{si} < P_{\text{sref}i} \end{cases} \tag{5}$$

It can be written in symbolic function form:

$$\omega_i = \frac{P_{\max i}}{\text{sign}(P_{\text{sref}i} - P_{si}) \cdot P_{si} + \left[1 - \text{sign}(P_{\text{sref}i} - P_{si})\right] \cdot P_{\max i} - P_{si}} \tag{6}$$

The maximization of capacity utilization rates of converters is achieved when power mismatches are shared proportionally to their available capacities Therefore, the objective function of sharing unbalanced power according to power margin is

$$\min \quad \omega_i (P_{\text{sref}i} - P_{si})^2 \tag{7}$$

3.3. Constraints

In order to meet the actual conditions of DC transmission system and the basic conditions of safe and stable operation, the optimization function needs to satisfy the constraints of droop control, capacity constraints of the converter and stability constraints of DC voltage.

Droop control constraint: the droop control equation of the converter.

$$K_{\text{droop}i}(U_{\text{dcref}} - U_{\text{dc}i}) + P_{\text{sref}i} - P_{si} = 0 \tag{8}$$

Converter capacity constraint: the output power of the converter cannot exceed its maximum capacity during system operation.

$$0 \leq P_{si} \leq P_{\max i} \tag{9}$$

DC voltage stability constraint: According to the voltage stability requirements, the DC voltage must not exceed 5% of the voltage reference value U_{dcref}.

 doi:10.20944/preprints202505.0544.v1

$$U_{\text{dcref}} \times 0.95 \le U_{\text{dc}i} \le U_{\text{dcref}} \times 1.05 \tag{10}$$

4. Cooperative Control Method Integrated with the Two-Objective Optimization Model

In HVDC systems, the cooperative control of multiple MMCs at the receiving end aims to achieve the comprehensive optimization of voltage deviation minimization and power mismatches sharing proportionally to their available capacities through global information interaction. In this section, a cooperative control strategy integrated the two-objective optimization model is proposed. The structure of the cooperative control strategy is shown in Figure 3, which consists of a central controller and the local controllers of each MMC. The communication and data interaction flow are as follows:

1) Data acquisition and uploading

Each MMC local controller collects the information of DC bus voltage and output power in real time and uploads them to the central controller.

2) Multi-objective optimization based cooperative control

When the system detects a fault or the power fluctuation exceeds the threshold, the optimization controller is triggered, and the system calculates the optimal power sharing and the optimal droop coefficient of the system based on the multi-objective optimization model through the GWO algorithm.

3) Optimization instruction issuance

The central controller sends the calculated optimization commands to each MMC and synchronously updates the current state of the system

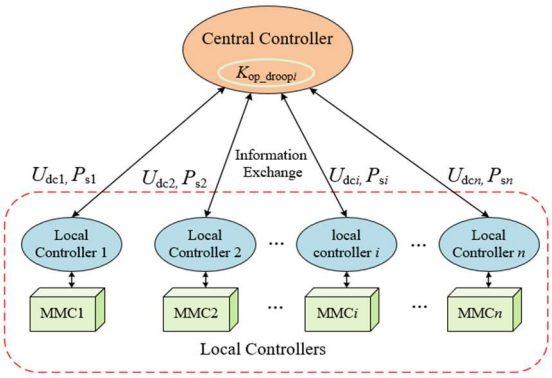

Figure 3. The structure of the cooperative control method.

4.1. Cooperative Control Method

Under multiple droop controllers, the objectives of voltage deviation minimization and capacity utilization rates maximization can be expressed as

$$f_1 = \min \sum_{i=1}^{n} (U_{\text{dcref}} - U_{\text{dc}i})^2 \tag{11}$$

$$f_2 = \min \sum_{i=1}^{n} \omega_i (P_{\text{sref}i} - P_{si})^2 \tag{12}$$

Therefore, combining the two objectives, the final expression of the optimization objective function can be written as

 doi:10.20944/preprints202505.0544.v1

$$\begin{aligned} F &= f_1 + f_2 \\ &= \min\left\{\sum_{i=1}^{n}((U_{\text{dcref}} - U_{\text{dc}i})^2 + \omega_i (P_{\text{sref}i} - P_{si})^2)\right\} \\ &= \min\left\{\sum_{i=1}^{n}((U_{\text{dcref}} - U_{\text{dc}i})^2 \right. \\ &\left. + \frac{P_{\max i}}{\text{sign}(P_{\text{sref}i} - P_{si}) \cdot P_{si} + [1 - \text{sign}(P_{\text{sref}i} - P_{si})] \cdot P_{\max i} - P_{si}} (P_{\text{sref}i} - P_{si})^2)\right\} \end{aligned} \tag{13}$$

It can be seen that when the power margin of the converter is larger, the power margin coefficient ω_i is smaller, and then the role of the power deviation term $(P_{\text{sref}i} - P_{si})^2$ in the objective function of the converter will be weakened, and the system will put the focus of the control objective of the converter on controlling the deviation of the DC voltage. On the contrary, when the power margin of the converter is smaller, the power margin coefficient ω_i is larger, and then the role of the power deviation term $(P_{\text{sref}i} - P_{si})^2$ in the objective function will be strengthened, and the system will put the focus of the control objective of the converter on the power sharing. function, the system will focus the control objective of the converter on power sharing. Adjusting the focus of the control objective of the converter through the power margin coefficient can well balance the two conflicting control objectives of voltage control and power control.

4.2. Solution of Cooperative Control

The multi-objective optimization model is a nonlinear planning problem with constraints, which is solved by using the Grey Wolf Algorithm (GWO), which can obtain $U_{\text{dc}i}$ and P_{si} when making the objective function reach the minimum, and then the optimal droop coefficients can be found through the droop control equation.

Mirjalili et al. [20]proposed the Grey Wolf Optimizer (GWO), a swarm intelligence optimization algorithm inspired by the social hierarchy and hunting behavior of grey wolves. The algorithm aims at wolf tracking, encircling, pursuing and attacking prey by mimicking the predatory strategy of wolves in order to achieve optimal search. In the GWO algorithm, each solution is regarded as a wolf, and the top 3 best wolves (optimal solutions) are defined as α, β, and δ. Define the remaining solutions as ω, which update their positions around α, β, and δ.

1. Surrounding the prey

Grey wolves encircle their prey during a hunt, expressing the encirclement behavior as

$$\boldsymbol{D} = \left|\boldsymbol{C}\boldsymbol{X}_P(t) - \boldsymbol{X}(t)\right| \tag{14}$$

$$\boldsymbol{X}(t+1) = \boldsymbol{X}_P(t) - \boldsymbol{A}\boldsymbol{D} \tag{15}$$

where $\boldsymbol{A}$ and $\boldsymbol{C}$ are the coefficient vectors, $\boldsymbol{D}$ is the current distance between the grey wolf and the prey, t is the number of iterations so far, $\boldsymbol{X}_P(t)$ and $\boldsymbol{X}(t)$ are the position vectors of the prey and the grey wolf, respectively, and $\boldsymbol{X}(t+1)$ is the update of the position of the grey wolf. The coefficient vectors $\boldsymbol{A}$ and $\boldsymbol{C}$ are calculated as follows:

$$\boldsymbol{A} = 2\boldsymbol{a} \cdot \boldsymbol{r}_1 - \boldsymbol{a} \tag{16}$$

$$\boldsymbol{C} = 2 \cdot \boldsymbol{r}_2 \tag{17}$$

 doi:10.20944/preprints202505.0544.v1

where α is the convergence factor that decreases linearly from 2 to 0 with the number of iterations, r_1 and r_2 obeys a uniform distribution between [0,1].

2. Hunting

In the GWO algorithm, the traveling direction of the whole wolf pack is jointly determined by the optimal three solutions α , β , δ and gradually approaching the prey. The mathematical model of the individual grey wolf tracking the location of the prey is described as follows

$$\begin{cases} \boldsymbol{D}_\alpha = \left| \boldsymbol{C}_1 \cdot \boldsymbol{X}_\alpha - \boldsymbol{X} \right| \\ \boldsymbol{D}_\beta = \left| \boldsymbol{C}_2 \cdot \boldsymbol{X}_\beta - \boldsymbol{X} \right| \\ \boldsymbol{D}_\delta = \left| \boldsymbol{C}_3 \cdot \boldsymbol{X}_\delta - \boldsymbol{X} \right| \end{cases} \tag{18}$$

where $\boldsymbol{D}_\alpha , \boldsymbol{D}_\beta , \boldsymbol{D}_\delta$ denote the distances between α 、 β 、 δ and other individuals, respectively; $\boldsymbol{X}_\alpha$, $\boldsymbol{X}_\beta$, $\boldsymbol{X}_\delta$ represent the current positions of α 、 β 、 δ respectively; $\boldsymbol{C}_1$ 、 $\boldsymbol{C}_2$ 、 $\boldsymbol{C}_3$ are random vectors, and $\boldsymbol{X}$ is the current position of the gray wolf.

$$\begin{cases} \boldsymbol{X}_1 = \boldsymbol{X}_\alpha - \boldsymbol{A}_1 \cdot (\boldsymbol{D}_\alpha) \\ \boldsymbol{X}_2 = \boldsymbol{X}_\beta - \boldsymbol{A}_2 \cdot (\boldsymbol{D}_\beta) \\ \boldsymbol{X}_3 = \boldsymbol{X}_\delta - \boldsymbol{A}_3 \cdot (\boldsymbol{D}_\delta) \end{cases} \tag{19}$$

$$\boldsymbol{X}(t+1) = \frac{\boldsymbol{X}_1 + \boldsymbol{X}_2 + \boldsymbol{X}_3}{3} \tag{20}$$

Eq. (19) represents the step length and direction of an individual ω in the wolf pack toward α 、 β 、 δ and Eq. (20) denotes the final position of ω .

In actual operation, the real-time optimization model monitors the system's operational state online. When power fluctuations or failures occur, it collects the voltage and power information for the current time period, compiles it into a cluster, and subsequently determines the optimal droop coefficient based on the optimization model described in the previous section. No optimization is performed when the system is in a stable operating state.

Figure 4. illustrates the optimization control flow of the system. When the system is initially in a stable operating state, the droop coefficients is initialized, and the fixed droop coefficients are applied. Upon detecting a fault or when power fluctuation exceeds the threshold, the cooperative optimization control strategy computes the optimal power sharing and droop coefficients for the system. The optimal droop coefficients are then assigned to the droop controllers, enabling state switching. Once the system recovers from the fault or the output power returns to a stable state, the optimal droop control strategy is withdrawn, and the system reverts to the fixed droop coefficient control strategy.

 doi:10.20944/preprints202505.0544.v1

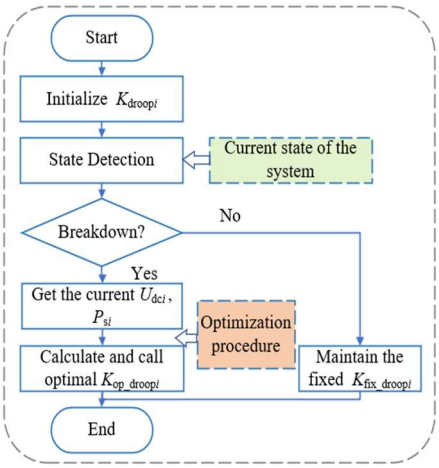

Figure 4. Flowchart of system optimized droop control.

5. Results

5.1. Simulation Model and Parameters

In PSCAD/EMTDC, the DC transmission system as shown in Fig. 1 is constructed, with four MMCs used for control at the receiving end. Among them, MMC1, as the main converter, adopts a fixed DC voltage control strategy; MMC2, MMC3, and MMC4 employ the droop control strategy, with steady-state active power reference values set to 300 MW, 400 MW, and 500 MW, respectively. The reference value for the DC voltage is set to 400 kV, and the fixed droop coefficients for all converters are set to 1.5. The simulation parameters of the system are provided in Table 1.

Table 1. System simulation parameters.

Parameters	Value
Rated voltage on AC side(kV)	500
Rated active power delivered by the line(MW)	4000
Rated frequency(Hz)	50
Total length of the line(km)	2100
Rated voltage on the DC side of MMC(kV)	400
Rated active capacity of MMC1(MW)	2000
Rated active capacity of MMC2(MW)	1000
Rated active capacity of MMC3(MW)	1000
Rated active capacity of MMC4(MW)	1000
Default droop coefficient	1.5
Active power reference for MMC2	300
Active power reference for MMC3	400
Active power reference for MMC4	500

5.2. System Performance Evaluation Index Setting

The DC voltage deviation evaluation index is the maximum deviation of DC voltage during fault or disturbance:

$$\Delta U_{\mathrm{dcmax}} = \left| U_{\mathrm{dcref}} - U_{\mathrm{dc}} \right|_{\max} \tag{21}$$

The power sharing evaluation index is the capacity utilization of the droop-controlled converters:

 doi:10.20944/preprints202505.0544.v1

$$\eta = \frac{\sum_{i=2}^{4} \frac{P_{si}}{P_{\max i}}}{3} \tag{22}$$

Obviously, the smaller the maximum deviation of DC voltage and the larger the capacity utilization of the droop-controlled converters, the better the system performance.

5.3. Case 1: The System Performance When the Converter MMC1 Is Out of Service

Normally, the active power output from the main converter MMC1 is relatively large, and if the control strategy is not appropriately designed, the sudden withdrawal of the converter from operation may cause fluctuations in the DC line voltage and power. This could also lead to overloading in the converter with a smaller power margin. To verify the effectiveness of the optimized droop control strategy proposed in this paper, the system is set to withdraw MMC1 from service at the 2nd second and resume operation at the 3rd second. Simulations are conducted using both the conventional fixed-droop control strategy and the synergistic optimized droop control strategy proposed herein, with the simulation results shown in Figure 5.

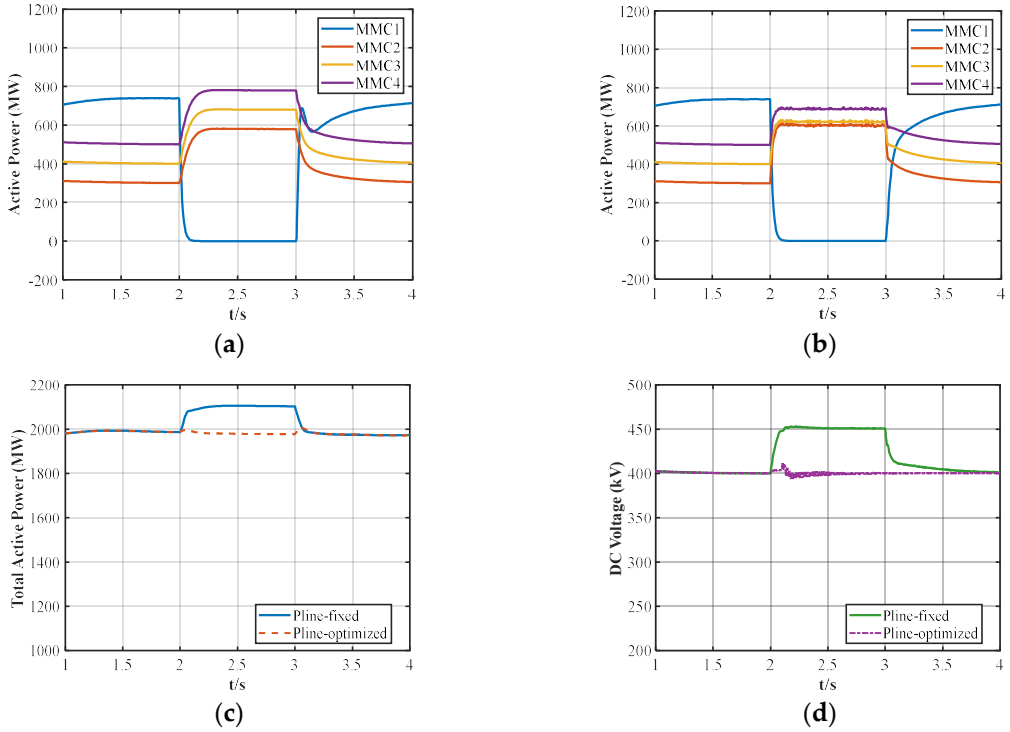

Figure 5. System simulation results when MMC1 is out of service.(a) Active power of MMCs under conventional droop control strategy; (b)Active power of MMCs under optimized droop control strategy; (c) the power at the common DC bus for MMCs ; (d) DC voltage.

As shown in Figure 5, when MMC1 is out of service, the power mismatches caused by MMC1 is equally shared among the three droop-controlled converters under the conventional droop control strategy. In contrast, the optimized droop control strategy enables the sharing of power in accordance with the available capacities of each converter. Specifically, MMC3 and MMC4, which have a larger power margin, bear more of the unbalanced power, while MMC2, with a smaller power margin, handles a relatively smaller portion of the power mismatches. Additionally, under the conventional droop control strategy, the power at the common DC bus for MMCs(total active power of MMCs) increases when MMC1 is out of operation, leading to system instability. However, under the optimized droop control strategy, the power at the common DC bus for MMCs remains stable.

 doi:10.20944/preprints202505.0544.v1

During the fault period (2~3s), the data in Figure 5 (d) show that the DC voltage deviation ΔU_{dcmax} is 51.73 kV under the conventional droop control strategy, while it is only 14.62 kV under the optimized droop control strategy, a reduction of 71.74%. Under the conventional droop control strategy, the DC voltage falls outside the stability range during the fault period, while under the optimized droop control strategy, the DC voltage experiences only minor fluctuations and remains stable.

5.4. Case 2: The System Performance When a Three-Phase Ground Fault at a Converter Occurs

In this paper, the effectiveness of the optimized droop control strategy is verified by applying a three-phase transient fault on the AC side of MMC1. A three-phase ground fault is introduced at the 2nd second, with a fault duration of 0.1 second. The conventional and optimized droop control strategies are applied, and the simulation results are shown in Figure 6.

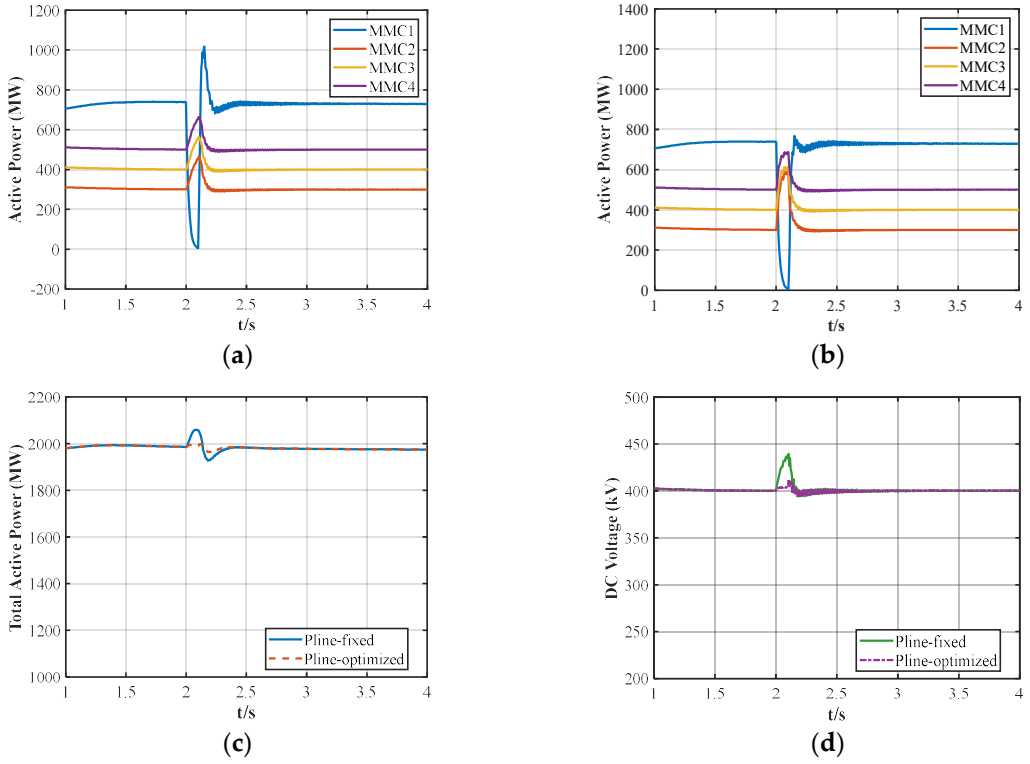

Figure 6. System simulation results when three-phase ground fault occurs in MMC1.(a) Active power of MMCs under conventional droop control strategy; (b)Active power of MMCs under optimized droop control strategy; (c) the power at the common DC bus for MMCs ; (d) DC voltage.

From Figure 6, it can be seen that under the conventional droop control strategy, due to the lack of adjustment of the droop coefficient, there is a power jump in MMC1 during fault recovery, which can lead to overloading of MMC1 and cause power fluctuations at the MMC converging bus. Additionally, the DC voltage falls outside the allowable range during the fault period, destabilizing the system. In contrast, when the optimized droop control strategy is adopted, the power remains stable during the fault recovery period, and the DC voltage stays within the allowable range, ensuring system stability. This stability is achieved through timely adjustment of the droop coefficient. During the fault period (2~2.5s), as shown in Figure 6 (d), it can be calculated that the DC voltage deviation ΔU_{dcmax} is 42.35kV with the conventional droop control strategy and 13.69kV with the optimized droop control strategy, representing a reduction of 67.67%.

 doi:10.20944/preprints202505.0544.v1

5.5. Case 3: The System Performance When Large Load Fluctuations Occur

In order to verify the effectiveness of the optimized droop strategy proposed in this paper under load-side power fluctuations, the output power of MMC1 is set to experience two significant power fluctuations at the 2nd and 3rd seconds, each lasting 0.2 seconds. The simulation results for both strategies are shown in Figure 7.

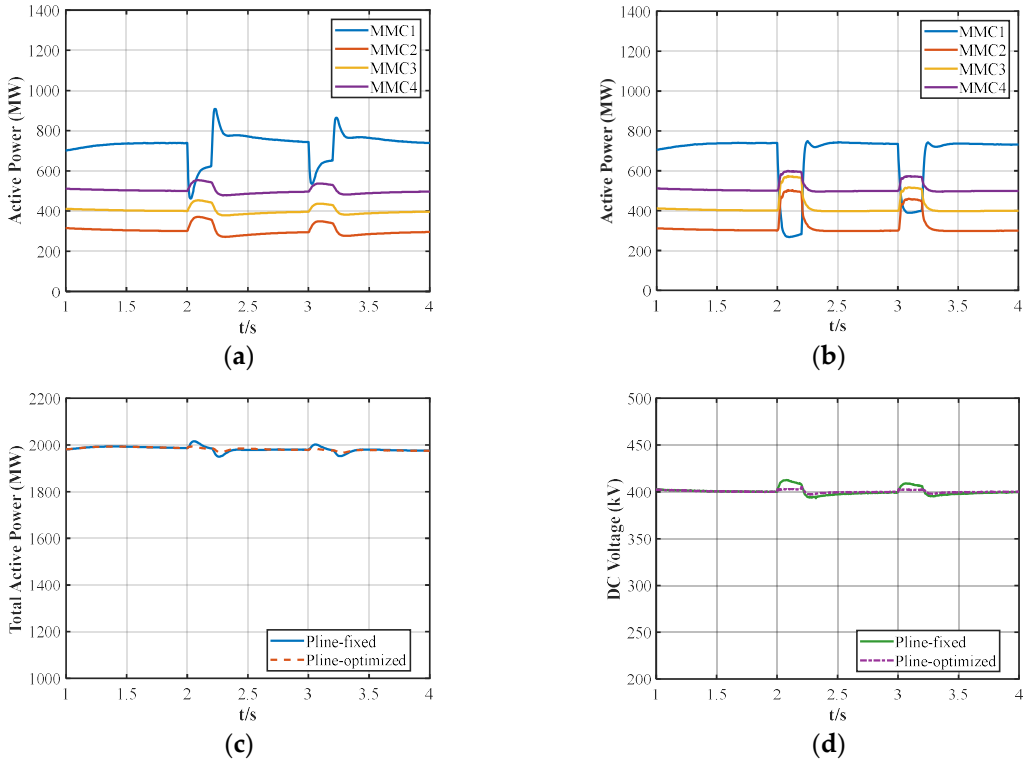

Figure 7. System simulation results when power fluctuation occurs in MMC1.(a) Active power of MMCs under conventional droop control strategy; (b)Active power of MMCs under optimized droop control strategy; (c) the power at the common DC bus for MMCs ; (d) DC voltage.

From Figure 7, it can be seen that under the conventional droop control strategy, the converter is unable to achieve stable system state transitions due to the influence of power perturbation. As a result, the output power of each converter and the power at the common DC bus for MMCs experience undesirable fluctuations, and the DC voltage remains insufficiently stable. In contrast, after adopting the optimized droop control strategy, the system can perform stable and rapid state switching, allowing the converter to quickly adapt to power changes, and the DC voltage remains more stable. During the two power fluctuations (2~2.5s and 3~3.5s), according to the data in Figure 7 (a) and (b), it can be calculated that the capacity utilization η under the conventional droop control strategy is 0.447 and 0.432, respectively, while the capacity utilization η under the optimized droop control strategy is 0.556 and 0.523, representing an improvement of 24.46% and 18.75%, respectively. This demonstrates that the optimized droop control strategy proposed in this paper enhances the performance of unbalanced power sharing during power fluctuations.

6. Conclusion

In this paper, a cooperative control method integrated with a multi-objective optimization model has been proposed to minimize voltage deviation and at the same time make power mismatches proportionate to their available capacities among converters. First, a two-objective optimization model is developed, which is a co-optimization of voltage deviation and power sharing among multiple converters. And then this optimization model is integrated to a cooperative control method,

 doi:10.20944/preprints202505.0544.v1

where the information of voltage and power among droop-controlled converters is acquired and the co-optimization of voltage deviation and power sharing is performed to obtain the optimal droop coefficients for these converters.

A testbed is established in PSCAD/EMTDC and simulations are carried out under different conditions. Compared to conventional droop control, the DC voltage deviation is reduced significantly by 71.74% and 67.67%, when a converter is out of service of and the three-phase ground fault occurs, respectively. Moreover, the capacity utilization rates of the droop-controlled converters increased by 24.46% and 18.75%, respectively.

Author Contributions: Conceptualization, J.L., J.Z. and Q.L.; methodology, J.L., J.Z. and Q.L.; software, J.L. and J.Z.; validation, Y.Z., K.W., P.G. and J.Z.; resources, J.K.Z.; data curation, J.L. and J.K.Z.; writing—original draft preparation, J.L., J.K.Z., Y.Z., K.W., P.G., J.Z. and Q.L.; writing—review and editing, J.L., J.K.Z., Y.Z., K.W., P.G., J.Z. and Q.L.; visualization, Y.Z. and J.Z.; supervision, Q.L.. All authors have read and agreed to the published version of the manuscript.

Funding: This research was funded by the Science & Technology Project of Northwest Branch of State Grid Corporation of China: Research on the stability and cooperative control methods for smart grids with high penetration of renewable energy sources under multi-type DC transmission modes (Grant No. SGNW0000DZJS2400152).

Data Availability Statement: The original contributions presented in this study are included in the article. Further inquiries can be directed to the corresponding author.

Acknowledgments: In this section, you can acknowledge any support given which is not covered by the author contribution or funding sections. This may include administrative and technical support, or donations in kind (e.g., materials used for experiments).

Conflicts of Interest: The authors declare that the research was conducted in the absence of any commercial or financial relationships that could be construed as a potential conflict of interest.

Abbreviations

The following abbreviations are used in this manuscript:

HVDC	High voltage direct current
LCC	Line commutated converter
MMC	Modular multilevel converter
GWO	Grey Wolf Optimizer

References

1. Li, X.; Xu, Z.; Zhang, Z. Application of MMC with embedded energy storage for overvoltage suppression and fault ride-through improvement in series LCC-MMC hybrid HVDC system. *Journal of Modern Power Systems and Clean Energy* **2022**, *11*, 1001-1013.
2. Liu, Z.; Lv, X.; Wu, F.; Li, Z. Multi-mode active inertia support strategy for MMC-HVDC systems considering the constraint of DC voltage fluctuations. *IEEE Transactions on Power Delivery* **2023**, *38*, 2767-2781.
3. Liu, Z.; Wang, Y.; Lai, J.; Zheng, A. Markov-based stochastic stabilization control for MMC-HVDC systems with inertia supporting under random disturbances. *IEEE Transactions on Power Systems* **2023**, *39*, 4077-4089.
4. Song, S.; Lei, J.; Ma, W.; Wang, Y. Kalman Filter Based Detection Scheme for DC-Link Voltage Measurement Faults in MMC-HVDC Systems. *IEEE Transactions on Power Electronics* **2024**.
5. Shen, H.; Dongye, Z.; Qi, L.; Wang, M.; Zhang, X.; Qiu, P.; Wei, X. Modeling of high-frequency electromagnetic oscillation for DC fault in MMC-HVDC systems. *CSEE Journal of Power and Energy Systems* **2022**, *9*, 1151-1160.

 doi:10.20944/preprints202505.0544.v1

6. Wang, C.; Xu, J.; Pan, X.; Gong, W.; Zhu, Z.; Xu, S. Impedance modeling and analysis of series-connected modular multilevel converter (MMC) and its comparative study with conventional MMC for HVDC applications. *IEEE Transactions on Power Delivery* **2021**, *37*, 3270-3281.
7. Hussaini, H.; Yang, T.; Gao, Y.; Wang, C.; Urrutia, M.; Bozhko, S. Optimal droop control design using artificial intelligent techniques for electric power systems of more-electric aircraft. *IEEE Transactions on Transportation Electrification* **2023**, *10*, 2192-2206.
8. Sekhavatmanesh, H.; Ferrari-Trecate, G.; Mastellone, S. Optimal adaptive droop design via a modified relaxation of the OPF. *IEEE Transactions on Control Systems Technology* **2022**, *31*, 497-510.
9. Wang, Y.; Qiu, F.; Liu, G.; Lei, M.; Yang, C.; Wang, C. Adaptive reference power based voltage droop control for VSC-MTDC systems. *Journal of Modern Power Systems and Clean Energy* **2021**, *11*, 381-388.
10. Liu, C.; Liu, H.; Jiang, S.; Zheng, L. Dynamic frequency support and DC voltage regulation approach for VSC-MTDC systems. *CSEE Journal of Power and Energy Systems* **2022**, *9*, 645-658.
11. Liu, Q.; Wang, Y.; Wang, S.; Liang, D.; Zhao, Q.; Zhao, X. Voltage regulation strategy for DC distribution networks based on coordination of centralized control and adaptive droop control. *IEEE Transactions on Power Delivery* **2021**, *37*, 3730-3739.
12. Sun, P.; Wang, Y.; Khalid, M.; Blasco-Gimenez, R.; Konstantinou, G. Steady-state power distribution in VSC-based MTDC systems and dc grids under mixed P/V and I/V droop control. *Electric Power Systems Research* **2023**, *214*, 108798.
13. Ye, Z.; Guo, C.; Liao, J.; Wang, Y. Improved droop control strategy for an MMC-MTDC connected to offshore wind farms with dynamic correction of the actual operating point. *International Journal of Electrical Power & Energy Systems* **2023**, *152*, 109277.
14. Beerten, J.; Belmans, R. Analysis of power sharing and voltage deviations in droop-controlled DC grids. *IEEE Transactions on Power Systems* **2013**, *28*, 4588-4597.
15. Gavriluta, C.; Candela, J.I.; Citro, C.; Rocabert, J.; Luna, A.; Rodríguez, P. Decentralized primary control of MTDC networks with energy storage and distributed generation. *IEEE Transactions on Industry Applications* **2014**, *50*, 4122-4131.
16. Wang, Z.; He, J.; Xu, Y.; Zhang, F. Distributed control of VSC-MTDC systems considering tradeoff between voltage regulation and power sharing. *IEEE Transactions on Power Systems* **2019**, *35*, 1812-1821.
17. Lee, W.-G.; Kim, H.-M. Deep Reinforcement Learning-Based Dynamic Droop Control Strategy for Real-Time Optimal Operation and Frequency Regulation. *IEEE Transactions on Sustainable Energy* **2024**, *6*, 284-294.
18. Gabl, O.M.A.; Shaaban, M.F.; Zeineldin, H.H.; Ammar, M.E. A multiobjective secondary control approach for optimal design of DG droop characteristic and control mode for autonomous microgrids. *IEEE Systems Journal* **2021**, *16*, 5445-5454.
19. Zhang, Y.; Shotorbani, A.M.; Wang, L.; Li, W. A combined hierarchical and autonomous DC grid control for proportional power sharing with minimized voltage variation and transmission loss. *IEEE Transactions on Power Delivery* **2021**, *37*, 3213-3224.
20. Mirjalili, S.; Mirjalili, S.M.; Lewis, A. Grey wolf optimizer. *Advances in engineering software* **2014**, *69*, 46-61.